Frontiers of Information Technology & Electronic Engineering
www.jzus.zju.edu.cn; engineering.cae.cn; www.springerlink.com
ISSN 2095-9184 (print); ISSN 2095-9230 (online)
E-mail: jzus@zju.edu.cn

Improving the reconstruction efficiency of sparsity adaptive matching pursuit based on the Wilkinson matrix

Rasha SHOITAN†‡[1,2], Zaki NOSSAIR[2], I. I. IBRAHIM[2], Ahmed TOBAL[1]

[1]*Computer and Systems Department, Electronic Research Institute, Giza 12622, Egypt*

[2]*Electronics, Communications, and Computer Department, Helwan University, Cairo 11795, Egypt*

†E-mail: Rasha.shoitan@eri.sci.eg

Received Sept. 27, 2016; Revision accepted Mar. 21, 2017; Crosschecked Apr. 15, 2018

Abstract: Sparsity adaptive matching pursuit (SAMP) is a greedy reconstruction algorithm for compressive sensing signals. SAMP reconstructs signals without prior information of sparsity and presents better reconstruction performance for noisy signals compared to other greedy algorithms. However, SAMP still suffers from relatively poor reconstruction quality especially at high compression ratios. In the proposed research, the Wilkinson matrix is used as a sensing matrix to improve the reconstruction quality and to increase the compression ratio of the SAMP technique. Furthermore, the idea of block compressive sensing (BCS) is combined with the SAMP technique to improve the performance of the SAMP technique. Numerous simulations have been conducted to evaluate the proposed BCS-SAMP technique and to compare its results with those of several compressed sensing techniques. Simulation results show that the proposed BCS-SAMP technique improves the reconstruction quality by up to six decibels (dB) relative to the conventional SAMP technique. In addition, the reconstruction quality of the proposed BCS-SAMP is highly comparable to that of iterative techniques. Moreover, the computation time of the proposed BCS-SAMP is less than that of the iterative techniques, especially at lower measurement fractions.

Key words: Block compressive sensing; Sparsity adaptive matching pursuit; Greedy algorithm; Wilkinson matrix
https://doi.org/10.1631/FITEE.1601588 **CLC number:** TP311

1 Introduction

According to the Nyquist-Shannon theorem, the sampling rate of a signal must be at least twice the highest frequency in the signal. This often results in too many samples and high memory requirements. In the real world, many signals have sparse values or good estimates with sparse coefficients in some orthonormal basis, such as the discrete wavelet transform (DWT) and the fast Fourier transform (FFT). Compressed sensing (CS) aims to use this sparse property and represents a signal using a small number of linear nonadaptive measurements. Specifically, CS compresses the signal at the time of sampling while maintaining the ability to reconstruct the original signal. Thus, it effectively reduces complexity and the cost of acquisition systems, in addition to recovering the sparse signal exactly by sampling at a sub-Nyquist rate (Candès, 2006; Donoho, 2006).

A wide variety of existing approaches can recover a sparse signal from a small number of linear measurements. Some techniques are linear programming and greedy algorithms (Stanković et al., 2012). In recent years, the recovery approaches, which are based on greedy algorithms, have received considerable attention (Needell et al., 2008). They have been widely applied in many applications because of their simple structure, easy implementation, and low reconstruction complexity. These greedy algorithms include matching pursuit (MP)

‡ Corresponding author
ORCID: Rasha SHOITAN, http://orcid.org/0000-0003-0372-4293

(Blumensath and Davies, 2008), orthogonal matching pursuit (OMP) (Tropp and Gilbert, 2007), stagewise OMP (StOMP) (Donoho et al., 2012), regularized orthogonal matching pursuit (ROMP) (Needell and Vershynin, 2010), and compressive sampling matching pursuit (CoSaMP) (Needell and Tropp, 2009). However, the major problem of these greedy algorithms is that they need prior information about the signal sparsity. Moreover, this problem constrains the applications of these algorithms in many fields such as image processing because the signal sparsity is unknown. Do et al. (2008) presented a new greedy algorithm called 'sparsity adaptive matching pursuit (SAMP)', to reconstruct the signal without prior information of the sparsity. However, SAMP suffers from high computational complexity and low reconstruction quality, especially at high compression ratios. Ma et al. (2011) presented a new fast SAMP (FSAMP) algorithm to reduce the redundant calculation of the SAMP technique. In the FSAMP algorithm, the updating of the support set is performed only once (when the support set expands) such that the algorithm can converge faster. Therefore, the complexity is greatly reduced.

Zhao et al. (2012) presented an improved SAMP algorithm based on regularized backtracking (SAMP-RB) to improve the reconstruction quality and to reduce the computation time. The SAMP-RB algorithm combines the most obvious advantages of SAMP and adopts a new idea of regularized backtracking method for the selection of atoms (columns).

In this study, we improve the efficiency of the SAMP technique by modifying the encoding side. Because choosing a good measurement matrix plays a vital role in improving the reconstruction quality, a new structured Wilkinson matrix is proposed as the measurement matrix. It improves the reconstruction quality and reduces the computation time of SAMP. On the other hand, the idea of dividing the image into blocks, which is called 'block compressive sensing (BCS)', is used, instead of applying the measurement matrix to the whole image to further reduce the computation time (Gan, 2007). Thus, the use of the Wilkinson matrix and the BCS overcomes the main disadvantages of the SAMP reconstruction technique.

2 Related work

2.1 Overview of compressive sensing

For a signal $\boldsymbol{x} \in \mathbb{R}^N$ that has at most k ($k \ll N$) nonzero components, we can obtain the compressed signal $\boldsymbol{y}$ with length M ($M < N$) through the linear transformation $\boldsymbol{y} = \boldsymbol{\Phi x}$, where $\boldsymbol{\Phi} \in \mathbb{R}^{M \times N}$. Therefore, the acquisition of M measurements instead of N values leads to a compression ratio of $(1-M/N)$. Because the number of unknowns is much larger than the number of observations, reconstructing $\boldsymbol{x}$ from the measurements $\boldsymbol{y} = \boldsymbol{\Phi x}$ corresponds to solving an under-determined set of linear equations. This means that the estimation of $\boldsymbol{x}$ is generally an ill-posed problem. If, however, the signal $\boldsymbol{x}$ is known to be sparse, there exists—under certain conditions—a unique solution and this is the fundamental tenet of the CS theory.

The goal of CS recovery is to find the sparsest possible solution that satisfies $\boldsymbol{y} = \boldsymbol{\Phi x}$. This optimization problem can be formulated as follows:

$$\min \ \|\boldsymbol{x}\|_0 \ \text{ s.t. } \ \boldsymbol{y} = \boldsymbol{\Phi x}, \tag{1}$$

where $\|\cdot\|_0$ indicates the ℓ_0 norm that counts the number of nonzero components of $\boldsymbol{x}$. Note that most natural signals are not sparse in the space domain, but are sparse in another transform domain, e.g., the Fourier transform, discrete cosine transform (DCT), and discrete wavelet transform (DWT). In such cases, the notation changes to $\boldsymbol{y} = \boldsymbol{\Phi x} = \boldsymbol{\Phi\Psi\alpha} = \boldsymbol{\theta\alpha}$, where $\boldsymbol{\Psi}$ is called the 'sparsifying transform'. The optimization problem becomes

$$\min \ \|\boldsymbol{\alpha}\|_0 \ \text{ s.t. } \ \boldsymbol{y} = \boldsymbol{\Phi\Psi\alpha} = \boldsymbol{\theta\alpha}. \tag{2}$$

Generally, the optimization problems (1) and (2) are nondeterministic polynomial time (NP) hard and need a combinatorial search through any possible sparse signal $\boldsymbol{x}$. Candès (2006) and Donoho (2006) first provided the basis pursuit algorithm to find the accurate approximation by relaxing the non-convex ℓ_0 optimization to a convex optimization problem such as ℓ_1 minimization, and the optimization problem becomes

$$\min \ \|\boldsymbol{\alpha}\|_1 \ \text{ s.t. } \ \boldsymbol{y} = \boldsymbol{\theta\alpha}. \tag{3}$$

The convex minimization problem can be solved using linear programming methods. Linear programming methods have shown to be effective in solving

such problems with high accuracy. However, in many applications that involve very high dimensional processing, linear programming methods are not optimally fast because their complexity grows in a cubic way in terms of the problem dimension N (Qaisar et al., 2013). Thus, more efficient algorithms that require a smaller number of iterations or less computation time per iteration are preferred, e.g., greedy algorithms, which compute the support of sparse signal $\boldsymbol{x}$ iteratively. Once the support of the signal is computed correctly, the pseudo-inverse of the selected columns of the measurement matrix is used to reconstruct the actual signal $\boldsymbol{x}$ (Zhang et al., 2015).

To guarantee that linear programming and greedy algorithms can reconstruct the k-sparse signal $\boldsymbol{\alpha}$ well, it is needed to prove that $\boldsymbol{\Phi}$ and $\boldsymbol{\Psi}$ are incoherent and that their product $\boldsymbol{\theta} = \boldsymbol{\Phi\Psi}$ satisfies the restricted isometry property (RIP) (Candès and Wakin, 2008; Pawar et al., 2015; Tiwari et al., 2015). When this property holds, it means that all subsets of k columns taken from $\boldsymbol{\theta}$ are in fact nearly orthogonal. Although the RIP is a useful property for describing how well the sensing matrix works, it is almost impossible to compute the RIP for any matrix. All subsets of k columns of the matrix should be tested and this is computationally difficult. One of the suitable ways is to measure the coherence between $\boldsymbol{\Phi}$ and $\boldsymbol{\Psi}$ (called mutual coherence) by looking at the columns of $\boldsymbol{\theta} = \boldsymbol{\Phi\Psi}$. Mutual coherence is defined as the largest absolute and normalized inner product between different columns in $\boldsymbol{\theta}$ as follows (Candès and Wakin, 2008):

$$\mu(\boldsymbol{\theta}) = \max_{1\le i,j\le N, i\neq j} \frac{\boldsymbol{\theta}_i^{\mathrm{T}}\boldsymbol{\theta}_j}{\|\boldsymbol{\theta}_i\|\|\boldsymbol{\theta}_j\|}. \tag{4}$$

The less coherent the columns of $\boldsymbol{\theta}$ are, the better the reconstruction works, because any two closely related columns may confuse any reconstruction technique. According to the smallest coherence principle, it is proved that the entries of the random observation matrices, such as the Gaussian random matrix and the Bernoulli matrix with independent and identical distribution, are almost universally incoherent (Candès et al., 2006). However, achieving these random matrices in practical applications has very high computational complexity and requires large storage capacity due to their inherent random structure. Later, many studies have reported several families of random measurement ensembles that behave equivalently, including partial FFT (Candès et al., 2006; Do et al., 2012; Shalaby et al., 2016), partial Walsh transform (Cai et al., 2013), and partial DCT (Do et al., 2012). The advantage of these partial transforms is that they are faster than random matrices while still possessing the RIP and coherence properties (Tiwari et al., 2015). In this study, the Wilkinson matrix is proposed as a measurement matrix, and it is applied on small blocks of an image to speed up the reconstruction process, enhance the quality of the reconstructed image, and increase the compression ratio.

2.2 Sparsity adaptive matching pursuit

SAMP is one of the greedy algorithms that compute the support of the sparse signal $\boldsymbol{x}$ iteratively. The basic structure of the SAMP technique is given in Fig. 1. SAMP uses the 'divide and conquer' principle stage by stage to estimate the sparsity level and the true support set of the target signals. SAMP applies two tests to build the estimated signal's set (called the 'finalist'). These two tests are called the 'preliminary test' and 'final test', respectively. The preliminary test is used to choose the largest elements corresponding to the largest values of correlation between the residual and the measurement matrix. After the preliminary test, a candidate list is created by the union of the chosen list in the preliminary test and the finalist in the previous iteration. The final test first solves a least-square problem and then chooses from the candidate list a subset of Γ coordinates that correspond to the largest entries in magnitude of the least-square solution. This subset of coordinates serves as the finalist. The residual is finally updated by subtracting the measured vector $\boldsymbol{y}$ from its projection onto the subspace spanned by the columns in the finalist. The remarkable innovation of SAMP is the backtracking technique in its final test. This enables the algorithm to remove wrong coordinates added in the previous iteration (Do et al., 2008).

Algorithm 1 summarizes the steps of the SAMP algorithm (Do et al., 2008; Zhao et al., 2012).

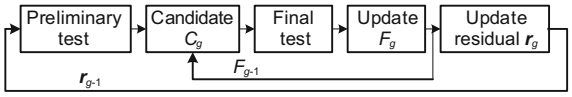

Fig. 1 Basic structure of the sparsity adaptive matching pursuit (SAMP) technique

Algorithm 1 Sparsity adaptive matching pursuit algorithm

Input: compressed signal $\boldsymbol{y}$; measurement matrix $\boldsymbol{\Phi}$; fixed increase units for step size; stopping criterion.

Initialization: initial residual $\boldsymbol{r}_0=\boldsymbol{y}$; finalist set $F_0=\phi$; initial step size $\Gamma=s$; let $g=1$ and $j=1$, where g is the iteration index and j is the stage index.

1: Find candidate set S_g by choosing Γ largest columns in the absolute value of $\langle \boldsymbol{r}_{g-1}, \boldsymbol{\Phi}\rangle$ (preliminary test).
2: Obtain the candidate set by $C_g=F_{g-1}\cup S_g$.
3: Compute $\tilde{\boldsymbol{x}}_{C_g}=\tilde{\boldsymbol{\Phi}}_{C_g}^{\dagger}\boldsymbol{y}$ and choose the Γ largest columns in the value of $\tilde{\boldsymbol{x}}_{C_g}$.
4: Select the finalist set F by choosing the atoms from C_g corresponding to the Γ largest atoms in the value of $\tilde{\boldsymbol{x}}_{C_g}$ (final test).
5: Compute $\boldsymbol{r}=\boldsymbol{y}-\boldsymbol{\Phi}_F\tilde{\boldsymbol{\Phi}}_F^{\dagger}\boldsymbol{y}$.
6: If $\|\boldsymbol{r}\|\geq\|\boldsymbol{r}_{g-1}\|$, then update $j=j+1$, $\Gamma=js$, and $g=1$, and go to step 7; otherwise, update $F_g=F$, $\boldsymbol{r}_g=\boldsymbol{r}$, and $g=g+1$, and go to step 7 to continue a new stage of iteration.
7: If $\|\boldsymbol{r}\|\leq\varepsilon$, we obtain the final solution $\tilde{\boldsymbol{x}}=\tilde{\boldsymbol{\Phi}}_F^{\dagger}\boldsymbol{y}$; otherwise, go to step 1.

Output: approximation vector $\boldsymbol{x}$.

The SAMP algorithm approaches the sparsity of the signal by accumulating the step size Γ with a fixed unit s. Thus, Γ changes at each stage. The finalist F is increased automatically with the change of Γ. The step size in the SAMP algorithm is required to be smaller than k. However, there is a trade-off between s and the recovery speed, since a smaller value of s requires more iterations. Empirical results suggest that a small s is preferable for signals with exponentially decayed magnitude, while a large s is advantageous for binary sparse signals. The derivation of the optimal value for s remains an open question.

2.3 Conventional CS based on the SAMP technique

The basic structure of the conventional CS based on the SAMP technique is illustrated in Fig. 2. As mentioned in Section 2.2, the main advantage of the SAMP algorithm is that it can reconstruct the signal without prior information about the sparsity. Therefore, the CS paradigm exploits the SAMP reconstruction technique in its decoding side. Because the SAMP requires the signals to be sparse, the image is transformed into a sparse signal using two decomposition levels of the forward discrete wavelet transform (FDWT). In addition, the measurement matrix used in this CS paradigm is the DCT matrix (Do et al., 2008).

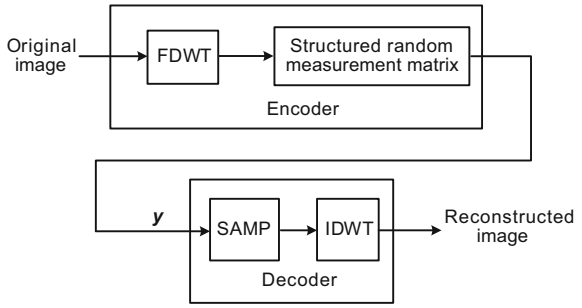

Fig. 2 Basic structure of the conventional compressed sensing (CS) based on the sparsity adaptive matching pursuit (SAMP) technique

The drawback of this CS paradigm is that SAMP is more complex than the other greedy algorithms and it needs more time to reconstruct images. In addition, the images reconstructed by SAMP suffer from relatively poor reconstruction quality, especially at higher compression ratios.

3 Proposed block compressive sensing-sparsity adaptive matching pursuit (BCS-SAMP) technique

In this study, the BCS-SAMP technique based on the Wilkinson matrix is proposed to improve the performance of the SAMP technique. From all previous compressive sensing research, it was found that choosing a good measurement matrix can improve the performance of any reconstruction algorithm. Therefore, the proposed method uses the Wilkinson matrix as the measurement matrix to improve the reconstruction efficiency of the SAMP technique. Fig. 3 summarizes the structure of the proposed BCS-SAMP technique, and its detailed information is explained in the following subsections.

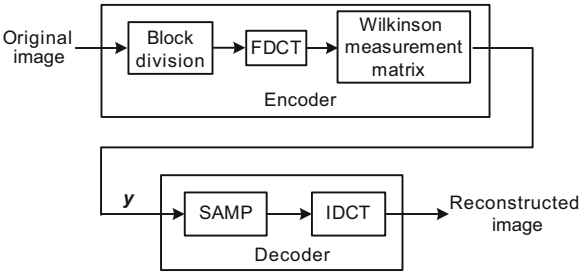

Fig. 3 Basic structure of the proposed block compressive sensing-sparsity adaptive matching pursuit (BCS-SAMP) technique

3.1 Wilkinson matrix

The Wilkinson matrix is a symmetric tridiagonal matrix (Fig. 4). This matrix is used for testing algorithms for computing eigenvalues (Gentle, 2007). The two largest eigenvalues of a Wilkinson matrix are nearly equal, and other pairs are almost equal to each other. The advantage of using this matrix in our proposed technique is that after taking M rows from it and reorthogonalizing these M rows, the resultant matrix will have many columns with zero values. As the number of M measurements decreases, the number of columns with zero values increases. These zero columns are at the end of the matrix, and this is considered the second advantage of using this matrix in our proposed technique. Fig. 5a shows an 8×8 Wilkinson matrix, and Fig. 5b shows the results of the orthogonalization of three rows from this Wilkinson matrix.

$\frac{n-1}{2}$	1	0	0	0	0	0	0	0
1	$\frac{n-2}{2}$	1	0	0	0	0	0	0
0	1	$\frac{n-3}{2}$	1	0	0	0	0	0
0	0	⋱	⋱	⋱	⋱	⋱	⋱	0
⋮	⋱	⋱	⋱	⋱	⋱	⋱	⋱	⋮
0	0	0	⋱	⋱	⋱	⋱	⋱	0
0	0	0	0	0	1	$\frac{n-3}{2}$	1	0
0	0	0	0	0	0	1	$\frac{n-2}{2}$	1
0	0	0	0	0	0	0	1	$\frac{n-1}{2}$

Fig. 4 Structure of the Wilkinson matrix

3.5	1	0	0	0	0	0	0
1	2.5	1	0	0	0	0	0
0	1	1.5	1	0	0	0	0
0	0	1	0.5	1	0	0	0
0	0	0	1	0.5	1	0	0
0	0	0	0	1	1.5	1	0
0	0	0	0	0	1	2.5	1
0	0	0	0	0	0	1	3.5

(a)

−0.78	0.58	−0.21	−0.05	0	0	0	0
−0.57	0.53	0.57	0.25	0	0	0	0
−0.23	0.54	−0.44	−0.68	0	0	0	0

(b)

Fig. 5 An 8×8 Wilkinson matrix (a) and results of the reorthgonalization of three rows from this Wilkinson matrix (b)

3.2 Description of the proposed BCS-SAMP technique

As mentioned in Section 2.2, at each iteration, SAMP searches for those columns of the measurement matrix that are most strongly correlated with the remaining part of the residual, and estimates the signal using two tests.

However, if the measurement matrix and the sparsity transform are not incoherent enough, this will produce a less representative measurement vector $\boldsymbol{y}$ and will mislead the SAMP search to the lack of reconstruction quality. Therefore, SAMP needs more iterations to reach the halting criterion and consumes more time. In the proposed BCS-SAMP technique, the forward DCT (FDCT) is used as a sparsity transform and the Wilkinson matrix is used as a measurement matrix. As is known, the top-left elements of a two-dimensional DCT matrix contain values that are almost always of a very great magnitude, and entries with increasing vertical and horizontal index values represent higher vertical and horizontal frequencies that contain less information and can be discarded.

As mentioned in Section 3.1, the high-order columns of the Wilkinson matrix are of zero values. Therefore, the algorithm will consider only the low-order DCT coefficients and discard the high-order coefficients. This will make the measured vector $\boldsymbol{y}$ be a combination of the low-order columns of the Wilkinson measurement matrix and the low-order coefficients of the DCT. Therefore, the measured vector $\boldsymbol{y}$ will contain the most important information about the image. At the decoder, SAMP uses the measured vector $\boldsymbol{y}$ and the measurement matrix $\boldsymbol{\Phi}$ to reconstruct the DCT coefficients of $\boldsymbol{x}$. SAMP searches for a set of columns from $\boldsymbol{\Phi}$ that are most correlated with $\boldsymbol{y}$, and uses the backtracking approach to eliminate the wrong columns from the selected columns. The use of the Wilkinson matrix at the encoder will help SAMP find the columns that contribute most to the construction of $\boldsymbol{y}$. Thus, the reconstruction process in our proposed technique will include more information about the signal than that in the conventional SAMP technique, and will consume less time.

4 Evaluation metric

The peak signal-to-noise ratio (PSNR) is used to measure the quality of the reconstructed images relative to the original images. If the maximum pixel intensity is given as 'MAX', then the peak power is given as 'MAX^2'. All images here are expressed using 8-bit intensity values per pixel. The peak pixel power is thus 255^2. The noise power is expressed in terms of the mean-squared error (MSE) between the original and reconstructed images.

The MSE between reconstructed image $\boldsymbol{R}$ and its original image $\boldsymbol{O}$ of $M\times N$ pixels is given by the following equation:

$$\mathrm{MSE}=\frac{1}{MN}\sum_{i=0}^{M-1}\sum_{j=0}^{N-1}\big(\boldsymbol{O}(i,j)-\boldsymbol{R}(i,j)\big)^2. \quad (5)$$

The PSNR, usually expressed in decibels (dB), is thus given as follows (Grgić et al., 2004):

$$\mathrm{PSNR}=10\lg\left(\frac{\mathrm{MAX}^2}{\mathrm{MSE}}\right). \quad (6)$$

5 Simulation results

In this section, we present the results of the simulations conducted to evaluate the proposed BCS-SAMP technique and compare its performance with those of the BCS-OMP (Sermwuthisarn et al., 2009), SAMP, gradient projection for sparse reconstruction (GPSR) (Do et al., 2012), and BCS-SPL (Shoitan et al., 2017) techniques. The software of SAMP and GPSR is used as provided in the literature. The PSNR is used to evaluate and compare these techniques for five measurement fractions of 0.1, 0.2, 0.3, 0.4, and 0.5. Five different sets of test images are used for performance evaluation. These test images are the Barbara, Lenna, Boat, and Gold hill images of 512×512 pixels and the heart magnetic resonance imaging (MRI) image of 256×256 pixels. The heart MRI was obtained from the cardiac MRI perfusion dataset. These images are shown in Fig. 6.

In the BCS-OMP technique, the measurement matrix used is the noiselet while the sparsity transform used is the Haar wavelet transform. The BCS-SPL technique uses the hybrid wavelet matrix as a measurement matrix and the DWT as a sparsity transform. However, in the conventional CS based on the SAMP technique, the DCT matrix is used as a measurement matrix and the Daubechies 9/7 wavelet transform as a sparsity transform. The measurement matrix used in the GPSR technique is the block DCT matrix (BDCT), while the sparsity transform is the Daubechies 9/7 wavelet transform. In the proposed BCS-SAMP technique, the Wilkinson matrix is used as a measurement matrix and the DCT as a sparsity transform.

Fig. 6 Original test images: (a) Barbara; (b) Lenna; (c) Boat; (d) Gold hill; (e) heart MRI

The encoder in the proposed technique starts processing each input image by dividing the image into blocks of 64×64. The block size is determined according to several preliminary simulations.

After the proposed technique is developed, it is compared with the BCS-OMP, BCS-SPL, SAMP, and GPSR techniques. Table 1 summarizes the PSNR results of these techniques under different fractions of measurements $M=0.1,0.2,\ldots,0.5$, on five test images. Note that in Table 1, at measurement fraction 0.1, the proposed BCS-SAMP technique ameliorates the quality of the reconstructed image by 2–3 dB over BCS-OMP and SAMP, and by 2.5 dB over GPSR on Barbara, Boat, and Gold hill images. However, the proposed method produces reconstructed images with quality less than 0.9 dB compared to the iterative BCS-SPL technique. As for the Lenna image, the proposed method enhances the quality of the reconstructed image by 5 dB over BCS-OMP, 2 dB over SAMP, and 4 dB over GPSR. However, BCS-SPL still gives higher quality than the proposed method by 1 dB. As for the MRI image, the proposed BCS-SAMP improves the quality of the reconstructed image by 5 dB over BCS-OMP, 2 dB over SAMP, and 5 dB over GPSR, while the reconstruction results of the BCS-SPL and the proposed BCS-SAMP are approximately the same.

Table 1 Reconstruction results in terms of the peak signal-to-noise ratio (PSNR) and the processing time by different techniques under five different measurement fractions (M/N)

Image	Technique	PSNR (dB)					Processing time (s)				
		0.1	0.2	0.3	0.4	0.5	0.1	0.2	0.3	0.4	0.5
Barbara	BCS-OMP	20.20	19.86	21.02	22.58	24.08	41.54	50.20	66.33	80.88	100.00
	SAMP	20.94	22.68	24.93	27.76	30.05	7.60	8.30	9.57	9.80	11.18
	GPSR (BDCT)	19.80	22.20	24.55	27.04	29.59	23.06	21.52	18.85	16.26	12.33
	BCS-SPL	**23.42**	25.02	27.15	29.69	33.87	13.06	19.66	19.34	22.03	15.71
	Proposed BCS-SAMP	22.98	**25.26**	**27.73**	**31.09**	**36.01**	**5.62**	10.47	18.67	38.73	61.45
Lenna	BCS-OMP	22.67	22.20	23.48	26.19	27.00	45.40	56.52	65.01	75.54	87.26
	SAMP	25.89	28.47	32.00	33.93	35.33	7.39	8.10	9.00	9.43	10.13
	GPSR (BDCT)	23.73	27.65	30.70	33.11	35.33	23.62	20.16	16.45	13.85	10.88
	BCS-SPL	**28.27**	**32.29**	**35.25**	37.93	39.69	9.34	12.82	21.00	18.36	15.10
	Proposed BCS-SAMP	27.27	31.77	34.93	**37.95**	**40.04**	**5.71**	10.50	18.67	38.56	55.22
Gold hill	BCS-OMP	23.02	22.18	24.05	25.83	26.71	35.47	40.76	49.32	61.37	71.81
	SAMP	24.16	26.31	28.01	29.53	30.98	7.73	8.53	9.37	9.99	10.62
	GPSR (BDCT)	23.07	25.53	27.62	29.42	31.40	19.75	17.14	15.96	15.48	12.03
	BCS-SPL	**27.12**	**29.68**	**31.75**	**33.81**	35.04	10.02	11.93	13.97	18.52	15.27
	Proposed BCS-SAMP	26.22	29.44	31.57	33.76	**35.43**	**5.68**	10.50	18.86	41.65	62.22
Boat	BCS-OMP	21.14	20.16	22.08	23.99	24.63	35.30	40.12	45.46	53.50	59.45
	SAMP	22.80	25.61	27.86	29.75	31.35	7.74	7.91	8.99	10.35	10.69
	GPSR (BDCT)	21.49	24.47	26.89	29.11	31.31	24.04	21.28	18.66	14.85	13.41
	BCS-SPL	**25.46**	**29.42**	**32.51**	**35.55**	37.41	10.01	14.76	17.04	18.47	15.14
	Proposed BCS-SAMP	24.39	28.94	32.09	35.53	**38.08**	**5.67**	10.47	18.79	38.60	55.45
MRI	BCS-OMP	21.16	21.34	21.79	24.29	25.21	10.33	11.11	13.53	18.44	25.07
	SAMP	23.81	25.83	27.19	28.55	30.17	1.51	1.65	1.43	1.45	1.50
	GPSR (BDCT)	21.83	24.67	26.61	28.38	30.55	7.13	6.05	4.49	4.93	3.55
	BCS-SPL	**26.81**	29.48	**31.63**	34.28	36.84	9.01	12.78	23.38	20.28	17.51
	Proposed BCS-SAMP	26.23	**29.54**	31.62	**34.59**	**38.40**	**1.45**	2.68	4.70	9.64	13.85

Bold numbers denote the best results

At measurement fractions greater than 0.2, the proposed BCS-SAMP technique outperforms the BCS-OMP, SAMP, and GPSR techniques in terms of the PSNR on all the test images. However, the reconstruction quality of the BCS-SPL technique is still higher than that of BCS-SAMP by approximately 1 dB until a measurement fraction of 0.4. At measurement fraction 0.5, the proposed BCS-SAMP improves the quality of the reconstructed image by approximately 1–2 dB over BCS-SPL on all test images.

On the other hand, BCS-SAMP compares with the SAMP-RB and FSAMP techniques (mentioned in Section 1), according to the simulation results provided in the literature. The measurement matrix used in the SAMP-RB technique is the Gaussian matrix. However, the measurement matrix used in the FSAMP technique is a structurally random matrix. By comparing the simulation results of our proposed technique with those obtained with the SAMP-RB and FSAMP techniques proposed by Ma et al. (2011) and Zhao et al. (2012), it can be found that the proposed BCS-SAMP technique improves the quality of the reconstructed Lenna image by 6–11 dB over SAMP-RB and by 3.5–5.6 dB over FSAMP under the five measurement fractions of 0.1, 0.2, 0.3, 0.4, and 0.5. In addition, the proposed technique improves the quality of the reconstructed Barbara image by 3–9 dB over the SAMP-RB technique under these five measurement fractions.

Because computation time plays an important role in many applications, time has been chosen as the second factor to be compared between the proposed technique and the other techniques. Table 1 presents the computation time. The processing time of each technique is measured after running five times, and the average of these five runs is calculated to obtain reliable results.

In Table 1, the proposed technique has the least processing time under the three measurement fractions 0.1, 0.2, and 0.3 over BCS-SPL, BCS-OMP,

and GPSR techniques on all test images. However, the SAMP technique consumes less processing time than the proposed technique, especially at measurement fractions starting from 0.2. To visually compare the reconstructed images obtained using the proposed technique and other techniques, Figs. 7–12 show the portions of the reconstructed images of Barbara, Lenna, and Gold hill at measurement fractions 0.1 and 0.2.

From Figs. 7, 9, and 11, it can be perceived that at measurement fraction 0.1, the reconstructed images obtained from the BCS-OMP, SAMP, and GPSR techniques suffer from huge distortion. On the other hand, the reconstructed Barbara and Lenna images from the proposed and the conventional BCS-SPL techniques suffer from blocking artifact distortion, but their reconstructed images are more intelligible (persons in the images are more recognizable). However, their reconstructed Gold hill images suffer from blocking artifacts and less smoothness. At measurement fraction 0.2, for the Barbara, Lenna, and Gold hill images, the reconstructed images from BCS-OMP, SAMP, and GPSR still suffer from high distortion. In contrast, the images reconstructed using the proposed BCS-SAMP and BCS-SPL techniques are clear.

6 Conclusions

We have proposed a compressive sensing approach in which the Wilkinson measurement matrix is used to improve the overall performance of the SAMP reconstruction technique. The proposed method suggests dividing the images into small blocks to help achieve greater improvement of the performance of the proposed BCS-SAMP. It can be concluded from the experimental results that the proposed BCS-SAMP technique improves the reconstruction quality relative to the existing greedy algorithms (SAMP, BCS-OMP) and the gradient method

Fig. 7 Portions of the reconstructed Barbara images by five different reconstruction techniques at measurement fraction 0.1: (a) BCS-OMP; (b) SAMP; (c) GPSR (BDCT); (d) BCS-SPL; (e) proposed BCS-SAMP

Fig. 8 Portions of the reconstructed Barbara images by five different reconstruction techniques at measurement fraction 0.2: (a) BCS-OMP; (b) SAMP; (c) GPSR (BDCT); (d) BCS-SPL; (e) proposed BCS-SAMP

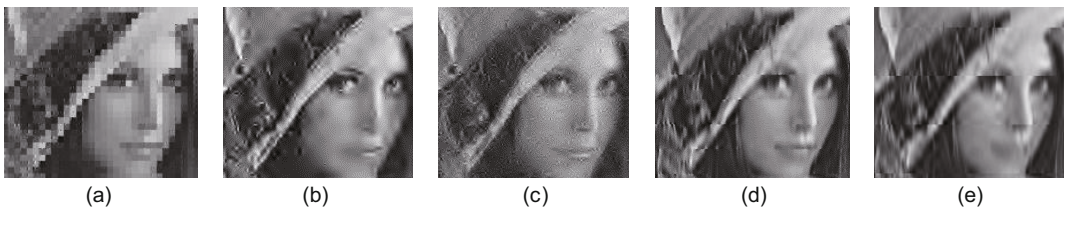

Fig. 9 Portions of the reconstructed Lenna images by five different reconstruction techniques at measurement fraction 0.1: (a) BCS-OMP; (b) SAMP; (c) GPSR (BDCT); (d) BCS-SPL; (e) proposed BCS-SAMP

Fig. 10 Portions of the reconstructed Lenna images by five different reconstruction techniques at measurement fraction 0.2: (a) BCS-OMP; (b) SAMP; (c) GPSR (BDCT); (d) BCS-SPL; (e) proposed BCS-SAMP

Fig. 11 Portions of the reconstructed Gold hill images by five different reconstruction techniques at measurement fraction 0.1: (a) BCS-OMP; (b) SAMP; (c) GPSR (BDCT); (d) BCS-SPL; (e) proposed BCS-SAMP

Fig. 12 Portions of the reconstructed Gold hill images by five different reconstruction techniques at measurement fraction 0.2: (a) BCS-OMP; (b) SAMP; (c) GPSR (BDCT); (d) BCS-SPL; (e) proposed BCS-SAMP

(GPSR). The proposed method reduces the computation time in comparison with BCS-OMP and GPSR for all measurement fractions, but SAMP still consumes less time than BCS-SAMP, especially at measurement fractions starting from 0.2. Moreover, the reconstruction efficiency of the proposed BCS-SAMP becomes comparable to the reconstruction efficiency of the iterative methods (BCS-SPL), especially at lower measurement fractions. In addition, the proposed method needs low computation time at very small measurement fractions compared to the iterative BCS-SPL technique.

References

Blumensath T, Davies ME, 2008. Gradient pursuits. *IEEE Trans Signal Process*, 56(6):2370-2382. https://doi.org/10.1109/TSP.2007.916124

Cai Z, Zhao H, Jia M, et al., 2013. An improved Hadamard measurement matrix based on Walsh code for compressive sensing. 9th Int Conf on Information, Communications, and Signal Processing, p.1-4. https://doi.org/10.1109/ICICS.2013.6782833

Candès EJ, 2006. Compressive sampling. Proc Int Congress of Mathematicians, p.1433-1452. https://doi.org/10.4171/022-3/69

Candès EJ, Wakin MB, 2008. An introduction to compressive sampling. *IEEE Signal Process Mag*, 25(2):21-30. https://doi.org/10.1109/MSP.2007.914731

Candès EJ, Romberg JK, Tao T, 2006. Stable signal recovery from incomplete and inaccurate measurements. *Commun Pure Appl Math*, 59(8):1207-1223. https://doi.org/10.1002/CPA.20124

Do TT, Gan L, Nguyen N, et al., 2008. Sparsity adaptive matching pursuit algorithm for practical compressed sensing. 42nd Asilomar Conf on Signals, Systems, and Computers, p.581-587. https://doi.org/10.1109/ACSSC.2008.5074472

Do TT, Gan L, Nguyen NH, et al., 2012. Fast and efficient compressive sensing using structurally random matrices. *IEEE Trans Signal Process*, 60(1):139-154. https://doi.org/10.1109/TSP.2011.2170977

Donoho DL, 2006. Compressed sensing. *IEEE Trans Inform Theory*, 52(4):1289-1306. https://doi.org/10.1109/TIT.2006.871582

Donoho DL, Tsaig Y, Drori I, et al., 2012. Sparse solution of under-determined systems of linear equations by stagewise orthogonal matching pursuit. *IEEE Trans Inform Theory*, 58(2):1094-1121. https://doi.org/10.1109/TIT.2011.2173241

Gan L, 2007. Block compressed sensing of natural images. 15th Int Conf on Digital Signal Processing, p.403-406. https://doi.org/10.1109/ICDSP.2007.4288604

Gentle JE, 2007. Matrix Algebra: Theory, Computations,

and Applications in Statistics. Springer Science & Business Media, New York, USA.

Grgić S, Grgić M, Mrak M, 2004. Reliability of objective picture quality measures. *J Electr Eng*, 55(1-2):3-10.

Ma CH, Xu CY, Shen L, et al., 2011. A fast sparsity adaptive matching pursuit algorithm for compressed sensing. In: Lee G (Ed.), Advances in Automation and Robotics, Vol. 1. Springer Berlin Heidelberg, p.363-368. https://doi.org/10.1007/978-3-642-25553-3_45

Needell D, Tropp JA, 2009. CoSaMP: iterative signal recovery from incomplete and inaccurate samples. *Appl Comput Harmon Anal*, 26(3):301-321. https://doi.org/10.1016/J.ACHA.2008.07.002

Needell D, Vershynin R, 2010. Signal recovery from incomplete and inaccurate measurements via regularized orthogonal matching pursuit. *IEEE J Sel Topics Signal Process*, 4(2):310-316. https://doi.org/10.1109/JSTSP.2010.2042412

Needell D, Tropp J, Vershynin R, 2008. Greedy signal recovery review. 42nd Asilomar Conf on Signals, Systems, and Computers, p.1048-1050. https://doi.org/10.1109/ACSSC.2008.5074572

Pawar K, Egan G, Zhang J, 2015. Multichannel compressive sensing MRI using noiselet encoding. *PLoS ONE*, 10(5):e0126386. https://doi.org/10.1371/journal.pone.0126386

Qaisar S, Bilal RM, Iqbal W, et al., 2013. Compressive sensing: from theory to applications, a survey. *J Commun Netw*, 15(5):443-456. https://doi.org/10.1109/JCN.2013.000083

Sermwuthisarn P, Auethavekiat S, Patanavijit V, 2009. A fast image recovery using compressive sensing technique with block based orthogonal matching pursuit. Int Symp on Intelligent Signal Processing and Communication Systems, p.212-215. https://doi.org/10.1109/ISPACS.2009.5383863

Shalaby WA, Saad W, Shokair M, et al., 2016. An efficient recovery algorithm using complex to real transformation of compressed sensing. 33rd National Radio Science Conf, p.122-131. https://doi.org/10.1109/NRSC.2016.7450845

Shoitan R, Nossair Z, Isamil I, et al., 2017. Hybrid wavelet measurement matrices for improving compressive imaging. *Signal Image Video Process*, 11(1):65-72. https://doi.org/10.1007/s11760-016-0894-5

Stanković S, Orović I, Sejdić E, 2012. Compressive sensing. In: Multimedia Signals and Systems. Springer, Boston, USA, p.285-348. https://doi.org/10.1007/978-1-4614-4208-0_6

Tiwari V, Bansod P, Kumar A, 2015. Designing sparse sensing matrix for compressive sensing to reconstruct high resolution medical images. *Cogent Eng*, 2(1):1017244. https://doi.org/10.1080/23311916.2015.1017244

Tropp JA, Gilbert AC, 2007. Signal recovery from random measurements via orthogonal matching pursuit. *IEEE Trans Inform Theory*, 53(12):4655-4666. https://doi.org/10.1109/TIT.2007.909108

Zhang Z, Xu Y, Yang J, et al., 2015. A survey of sparse representation: algorithms and applications. *IEEE Access*, 3:490-530. https://doi.org/10.1109/ACCESS.2015.2430359

Zhao R, Ren X, Han X, et al., 2012. An improved sparsity adaptive matching pursuit algorithm for compressive sensing based on regularized backtracking. *J Electron (China)*, 29(6):580-584. https://doi.org/10.1007/s11767-012-0880-1